On Climate Feedback Change and AMOC

Kai-Uwe Eiselt and Rune Grand Graversen
University of Tromsø

Contact Information:
Institute for Physics and Technology
University of Tromsø
Hansine Hansens Veg 18, Norway

Email: Kai-Uwe.Eiselt@uit.no

Abstract

Climate models disagree on climate response to greenhouse gas forcing. We employ a radiative kernel method to derive climate feedback decompositions for a range of members of phases 5 and 6 of the Coupled Model Intercomparison Project (CMIP) in the abrupt-4xCO2 experiment. Two model groups are distinguished according to their lapse-rate feedback change over time, one with small change (G1) and one with large change (G2). It is found that while G1 and G2 over time converge in terms of total feedback, their feedback decompositions become more different. Furthermore, particular regional differences between G1 and G2 are found in the Arctic and retraced to Arctic sea-ice evolution. Further differences in the evolution of the Atlantic Meridional Overturning Circulation (AMOC) and northern-hemispheric Hadley circulation are found and we suggest a causal connection to the global feedback change.

Introduction

In recent years it has become clear that the total climate feedback in numerical climate model experiments is not constant over time and this change of feedback over time is not consistent among models. However, the reasons for this are not yet understood. Current research indicates that shifting patterns of sea-surface warming may be the driver of the evolution of feedback over time, with the Indo-Pacific Warm Pool region appearing to exhibit particular influence (Dong et al., 2019). Here we analyse multiple models with respect to feedback change and present evidence that the Arctic may be another region of interest.

Materials and Methods

We use data from the CMIP phases 5 and 6 abrupt-4xCO2 experiments where the CO_2 concentration is increased by a factor of four in comparison to the pre-industrial equilibrium condition. All abrupt-4xCO2 experiments have a corresponding pre-industrial control experiment (piControl) and the changes are calculated with respect to this experiment. We apply a radiative kernel method (Soden et al., 2008) to derive individual climate feedbacks related to physical processes.

Results

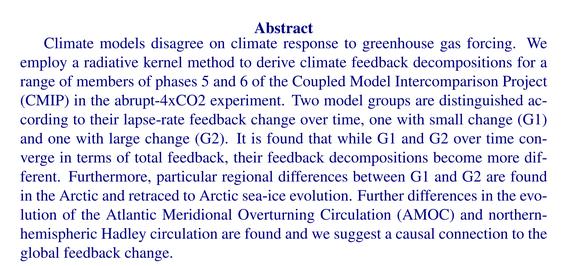

Figure 1: Gregory plots of individual kernel-derived feedbacks (left) and feedback sum (right) averaged separately over G1 and G2 (see text for details). Feedbacks are calculated as the regression of top-of-atmosphere radiative flux on surface-air temperature separately for early (subscript e; years 1–20) and late (subscript l; years 21–150) period. The radiative kernels were taken from Shell et al. (2008). Δ_{el} indicates the feedback difference between early and late period. LR stands for lapse rate, WV for water vapour, and SA for surface albedo.

Two Model Groups

The radiative kernel method was applied to 37 CMIP members. We use two thresholds to extract models into two groups: Models with weak global-mean lapse-rate (LR) feedback change (< 0.1 Wm^{-2}K^{-1}, G1) and models with strong global-mean LR feedback change (> 0.5 Wm^{-2}K^{-1}, G2).

Feedback and Feedback Change

Figure 1 (right) shows the Gregory plot of both model groups G1 and G2 (kernel-derived feedback sum). It is evident that while G2 has a larger feedback change over time, G1 exhibits stronger warming. The latter results from a less negative early-period total feedback in G1 than G2, while the late-period total feedbacks of G1 and G2 are similar. The feedback decomposition (Fig. 1, left) reveals that the difference in early feedback is mainly caused by the cloud feedback. However, the agreement of the late total feedback results mainly from changes in the LR feedback in G2.

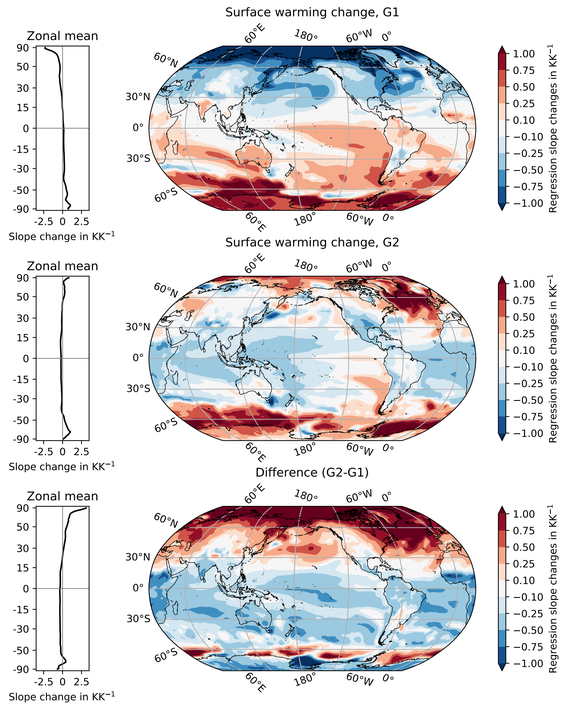

Figure 2: Maps and zonal means of surface-warming change relative to the global-mean change over time averaged over models with weak (upper, G1) and strong (middle, G2) lapse-rate feedback change as well as their difference (lower, G2−G1). The surface-warming change is calculated by first regressing local annual-mean surface temperature on global annual-mean surface temperature for the periods 1−20 (early) and 21−150 (late), and then subtracting results of early from late period. Note that the y-axis in the zonal-mean plot is scaled by the cosine of the latitude to obtain an equal-area perspective. See Eiselt and Graversen (2022).

Temperature Pattern Change

Figure 2 shows the change over time of local surface temperatures regressed on global mean surface temperature for G1 (top), G2 (middle) as well as G1 minus G2 (bottom). It is clear that the model groups are particularly different in the Arctic. This difference in Arctic warming is connected to Arctic sea-ice melt (see Fig. 5) and thus strong surface-albedo (SA) and LR feedback changes. How much these Arctic changes contribute to the global LR feedback change is not established here.

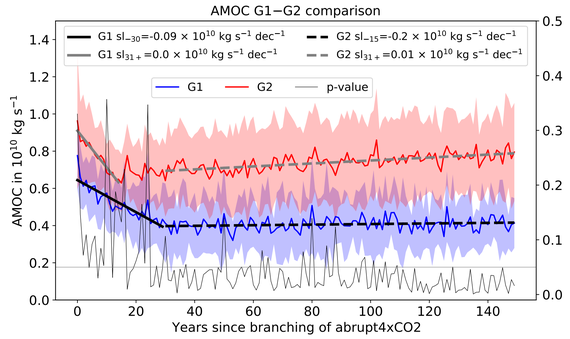

Figure 3: Atlantic meridional overturning circulation (AMOC) strength (calculated after Lin et al., 2019, but with a mixed-layer depth of 200 m). The lines indicate the multi-model means and the shading denotes the ±1-sigma spread. The black line shows the p-value of a two-sided Welch's t-test for the difference in group mean and the gray horizontal line indicates a p-value of 0.05. The subscripts -15, -30, and $31+$ denote regression periods 1–15, 1–30, and 41–150, respectively.

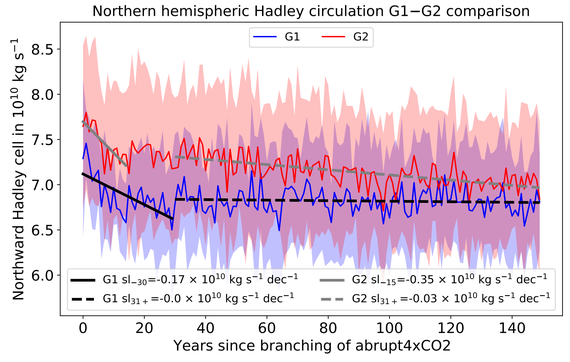

Figure 4: Northern-hemispheric Hadley circulation strength (calculated after Feldl and Bordoni, 2016). The lines indicate the multi-model means and the shading denotes the ±1-sigma spread. The subscripts -15, -30, and $41+$ denote regression periods 1–15, 1–30, and 41–150, respectively. See Eiselt and Graversen (2022).

AMOC and NH Hadley Circulation Change

Figure 3 shows the evolution of the AMOC in both model groups. It is clear that G2 initially has a stronger AMOC. In G1 the AMOC declines slower and over a longer time than in G2. However, the G1 AMOC remains constant after about 30 years of simulation, while the G2 AMOC only declines for about 15 years and then slightly recovers for the remainder of the simulation. It has recently been shown how changes of ocean heat transport (OHT) can influence climate sensitivity and feedback (Singh et al., 2022). Hence, the change in AMOC and its difference between G1 and G2 may be (in part) responsible for the difference in feedback change between G1 and G2. Singh et al. (2022) find that change in OHT is mostly compensated for by an opposite change in atmospheric energy transport (AET). However, here we find that early Hadley circulation is negative (Fig. 4), indicating that AET change, like OHT change, initially is negative. While it remains constant in G1 from year 30 on it further declines over the whole period for G2. The latter may be compensating the restrengthening of the AMOC and contribute to the constant Arctic amplification and continual sea-ice loss (Fig. 5) and thus a less negative late-period LR and a more positive late-period northern-hemispheric SA feedback in G2 compared to G1. In G1, sea ice is mostly lost by year 30, contributing (possibly together with OHT and AET being constant) to the declining Arctic amplification. However, the chain of causation needs further investigation.

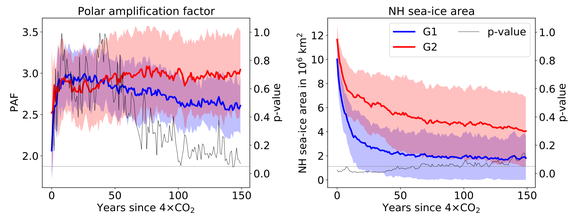

Figure 5: Polar amplification factor (PAF; left) and northern-hemispheric sea-ice area for G1 and G2 (see text for details). The PAF is calculated as the Arctic (75°–90°N) surface temperature anomaly divided by that of the global mean. The lines indicate the multi-model means, and the shading denotes the ±1-sigma spread. The black line shows the p-value of a two-sided Welch's t-test for the difference in group mean and the gray horizontal line indicates a p-value of 0.05. See Eiselt and Graversen (2022).

Conclusions

- Models with weak feedback change (G1) warm more than models with strong feedback change (G2).
- Early total feedback is different while late total feedback is similar between the two groups.
- The difference in early feedback is due to cloud feedback but the convergence of late feedback is due to a change in the LR feedback. Hence, feedback composition becomes more dissimilar over time.
- Differences between the model groups are prominent in the Arctic which may be connected to changes in AMOC and northern-hemispheric Hadley circulation. These changes may have causal influence on global LR feedback change. However, further research is needed to establish causality.

References

Dong, Y., C. Proistosescu, K. C. Armour, and D. S. Battisti (2019). "Attributing historical and future evolution of radiative feedbacks to regional warming patterns using a Green's function approach: The preeminence of the Western Pacific". In: *J. Climate* 32, pp. 5471–5491. DOI: 10.1175/JCLI-D-18-0843.1.

Eiselt, K.-U. and R. G. Graversen (2022). "Change in climate sensitivity and its dependence on lapse-rate feedback in 4xCO$_2$ climate model experiments". In: *J. Climate* 35, pp. 2919–2932. DOI: 10.1175/JCLI-D-21-0623.1.

Feldl, N. and S. Bordoni (2016). "Characterizing the Hadley circulation response through regional climate feedbacks". In: *J. Climate* 29, pp. 613–622. DOI: 10.1175/JCLI-D-15-0424.1.

Lin, Y.-J., Y.-T. Hwang, P. Ceppi, and J. M. Gregory (2019). "Uncertainty in the Evolution of Climate Feedback Traced to the Strength of the Atlantic Meridional Overturning Circulation". In: *Geophys. Res. Lett.* 46, pp. 12331–12339. DOI: 10.1029/2019GL083084.

Shell, K. M., J. T. Kiehl, and C. A. Shields (2008). "Using the Radiative Kernel Technique to Calculate Climate Feedbacks in NCAR's Community Atmospheric Model". In: *J. Climate* 21, pp. 2269–2282. DOI: 10.1175/2007JCLI2044.1.

Singh, H., N. Feldl, J. E. Kay, and A. E. Morrison (2022). "Climate sensitivity is sensitive to changes in ocean heat transport". In: *J. Climate* 35, pp. 2653–2674. DOI: 10.1175/JCLI-D-21-0674.1.

Soden, B. J., I. M. Held, R. Colman, K. M. Shell, J. T. Kiehl, and C. A. Shields (2008). "Quantifying climate feedbacks using radiative kernels". In: *J. Climate* 21, pp. 3504–3520. DOI: 10.1175/2007JCLI2110.1.